TYPE Original Research
PUBLISHED 24 November 2025
DOI 10.3389/feart.2025.1675908



OPEN ACCESS

EDITED BY Claudia Scatigno, Enrico Fermi Center for Study and Research, Italy

REVIEWED BY
Pavlo Maruschak,
Ternopil Ivan Pului National Technical
University, Ukraine
Osama A. Fouad,
Head of Nanostructured Materials and
Nanotechnology Department, Egypt
Joaquín Jiménez-Puerto,
University of Valencia, Spain

*CORRESPONDENCE Gloria Vaggelli, ☑ gloria.vaggelli@cnr.it

RECEIVED 29 July 2025 REVISED 26 September 2025 ACCEPTED 27 October 2025 PUBLISHED 24 November 2025

CITATION

Vaggelli G, Cossio R, Borghi A, Lippolis C and Ghignone S (2025) Geochemistry-based machine learning approach applied to an archaeological provenance study: the obsidian blades of Tulūl al-Baqarat (Iraq). *Front. Earth Sci.* 13:1675908. doi: 10.3389/feart.2025.1675908

COPYRIGHT

© 2025 Vaggelli, Cossio, Borghi, Lippolis and Ghignone. This is an open-access article distributed under the terms of the Creative Commons Attribution License (CC BY). The use, distribution or reproduction in other forums is permitted, provided the original author(s) and the copyright owner(s) are credited and that the original publication in this journal is cited, in accordance with accepted academic practice. No use, distribution or reproduction is permitted which does not comply with these terms.

Geochemistry-based machine learning approach applied to an archaeological provenance study: the obsidian blades of Tulūl al-Baqarat (Iraq)

Gloria Vaggelli¹*, Roberto Cossio², Alessandro Borghi², Carlo Lippolis³ and Stefano Ghignone²

¹Istituto di Geoscienze e Georisorse, Consiglio Nazionale delle Ricerche (CNR), Pisa, Italy, ²Dipartimento di Scienze della Terra, Università degli Studi di Torino, Turin, Italy, ³Dipartimento di Studi Storici, Università degli Studi di Torino, Turin, Italy

A machine learning approach was applied to geochemical analysis of nine obsidian blades discovered in the archaeological site of Tulūl al-Bagarat (4th millennium BCE, Iraq), aiming at unraveling the provenance of the natural material (volcanic glass, obsidian) employed for carving the studied tools. To accomplish this, we measured the geochemical composition of each archaeological tool to characterize the material, using non-invasive and non-destructive techniques. The obtained data were compared with other compositional data from obsidian sources in volcanic districts of the Near East in terms of major, minor, and trace elements. Significantly useful were the Zr and Rb minor elements, which have a remarkable discriminatory capacity in large volcanic contexts. To obtain more detailed discrimination, we also applied principal component analysis (PCA: covariate matrix) modeling and automatically compared these compositional data via a machine learning approach. Obsidian tools from Tulūl al-Baqarat show a rhyolitic composition and a geochemical fingerprint that allowed to exclude most obsidian outcrops in Turkish and Armenian volcanic sites as original sources, due to the different abundances of minor elements and PCA results. The most interesting outcome of our study indicates that obsidian blades resulted geochemically comparable to volcanic glasses from Nemrut Dağ stratovolcano (Southeastern Turkey), in accordance with the results (averaged probability) obtained via a machine learning approach. The possible provenance from Nemrut Dağ stratovolcano is remarkable because it is located on the Turkish route of the Tigris River, providing supporting evidence of a trade network and broad exchange activity since the 4th millennium BCE from Turkey and the south Near East to the shores of the Persian Gulf.

KEYWORDS

obsidian, provenance reconstruction, machine learning, Bingöl, Nemrut Dağ

1 Introduction

From the ancient Greek "opsdian" and the Latin "lapis obsidianus," obsidian is a volcanic rock derived from the rapid cooling of a degassed magma. Obsidian is an

excellent natural material for making artifacts with sharp edges by chipping. Due to its ideal physical properties, obsidian was widely used as raw material for making tools and items by prehistoric civilizations in the Near East and in the Mediterranean area (see, e.g., Chataigner et al., 1998; Bak et al., 2025).

The most common obsidian is black and has a rhyolitic composition ($SiO_2 > 70$ wt%), such as the famous "liparite," a black obsidian from Lipari (Aeolian Islands), widespread as raw material for carving prehistoric tools (Bigazzi and Bonadonna, 1993; Tykot, 1996).

This article presents an archaeometry study on a set of obsidian blades discovered in the archaeological site of Tulūl al-Baqarat (Wasit Province), approximately 25 km southwest of al-Kut in South-Central Iraq.

The aim of this study is to determine the provenance of the raw material (obsidian). To reach such an aim, we analyzed the archaeological tools using non-invasive and non-destructive techniques recommended for the study of archaeological tools (Birò, 2005). We used a low-vacuum SEM-EDS microprobe to determine major and minor elements and a bench-to-top micro-XRF for trace elements. The obtained data represent a detailed geochemical characterization (major, minor, and trace elements), used as a base for further comparisons. To avoid altering portions of the glass or the presence of small microlites, micro-analytical methods are preferred with respect to whole-rock chemical analysis (Frahm, 2012). Then, we compared our data with obsidian microchemical compositions from the literature via a machine learning approach. Major elements abundance allows classifying obsidians based on the main chemical composition, while trace element abundance represents the geochemical fingerprint fundamental to unravel different petrogenetic environments, likely unique for each volcanic source. Complete chemical compositions allow classification of different types of obsidian (classes) outcropping in several georeferenced volcanic sources (see, e.g., Frahm, 2012; Frahm, 2020; Khazaee et al., 2014; Frahm and Carolus, 2022).

2 Archaeological and volcanological settings

2.1 Tulūl al-Bagarat archaeological site

The studied tools belong to the Tulūl al-Baqarat archaeological site (Figure 1a), a rural settlement located 180 km southeast of Baghdad along the Tigris River, on the eastern margins of the Mesopotamian alluvium (Figure 1b). This region was home to well-known ancient civilizations due to its strategic location near water sources. In antiquity, the region of Tulūl al-Baqarat was probably situated closer to the course of the Tigris River or may have been connected to it via a system of canals. The settlement was continuously inhabited from the early 4th millennium BCE up until the Islamic era (Lippolis, 2020).

The archaeological site of Tulūl al-Baqarat is composed of a group of ten mounds, *tell* in Arabic (*tūlūl* plural). The main *tell* of the archaeological site is named TB1 (Tell Baqarat n. 1) and was extensively excavated from 2008 to 2010 by an Iraqi expedition with exceptional results (see Bahar, 2020; 2022). From 2013 to 2022, an Italian expedition (sponsored by the University of Turin and

the Centro Ricerche Archeologiche e Scavi di Torino) conducted soundings and a topographic survey on the main mounds of the area. In particular, they focused on a large low *tell* (average, 8 ha), named TB7 (Tell Baqarat n. 7, Figure 1a), located approximately 1 km to the southeast of TB1. The main architectural features and the materials (pottery, stone tools, flints, and clay-sickles) found in the TB7 *tell* suggest a settlement of a rural nature, with residential and productive units flanked by a monumental and raised sector (a building on a terrace?) in the middle of the *tell*.

The settlement, formerly circular in shape, was likely surrounded by a wide ditch, testified by a strong color change of the soil between the inner and the outer parts around TB7 (Lippolis et al., 2019).

TB7 architecture and other evidence point to dating the cultural layer to the main Early Uruk–Late Chalcolithic 2/3 period (4th millennium BCE). The later historical phases (e.g., the Parthian period) are poorly documented because of the strong erosion and land modifications that affected the site. Thus, TB7 contains the oldest evidence of human activity in the entire region (Lippolis, 2020).

Despite this, small fragments of painted pottery are attributed to the late Obeid period, or to a transitional phase between Obeid and Uruk periods (4th–5th millennium BCE). Obsidian tools studied in this article were found in the TB7 *tell*. These items are a set of prehistoric tools of daily life, such as blades and splinters (Lippolis, 2020).

Most of the obsidian tools found in the TB7 *tell* come from a collection of surface contexts. Although present in the investigated levels, obsidians in strata are rare compared to those encountered on the ground during a survey. It might be reasonable to claim that almost all the flints present in the *tell* can be attributed to the 4th millennium cultural horizon (Lippolis, 2020).

2.2 Volcanological setting of the eastern Anatolia region

There is extensive bibliography on the volcanoes of the Mediterranean and Near East regions, which reports the presence of obsidian-bearing volcanoes and volcanic obsidian deposits (Alıcı et al., 2001; Alpaslan, 2007; Azizi and Tsuboi, 2021; Di Giuseppe et al., 2018; Innocenti et al., 1976; Keskin, 2003; Keskin et al., 1998; Kurt et al., 2008; Lustrino et al., 2010; Lustrino et al., 2021; Pearce et al., 1990; Shaw et al., 2003; Yılmaz et al., 1998). In the Western Mediterranean area, obsidian sources are very few and relatively well studied, while in the Middle East, obsidian-bearing volcanoes cover hundreds of square kilometers and offer a wide range of investigation. Moreover, in addition to major obsidian source areas, small outcrops are scattered throughout Anatolia (Özdogan, 1994), making this area the most problematic for obsidian source identification (Oddone et al., 2003).

In addition, the obsidian sources for Tulūl al-Baqarat tools must be sought in an area easily accessible by ancient populations. In fact, Oddone et al. (2003) proposed sites reachable by foot or by river transport as the most suitable source areas, instead of the obsidian sources closest to the archaeological site (Tulūl al-Baqarat). Accordingly, we selected the eastern Anatolia region as the most suitable source area for the Tulūl al-Baqarat obsidian tools, focusing on the volcanic district near Lake Van (Kearney et al.,

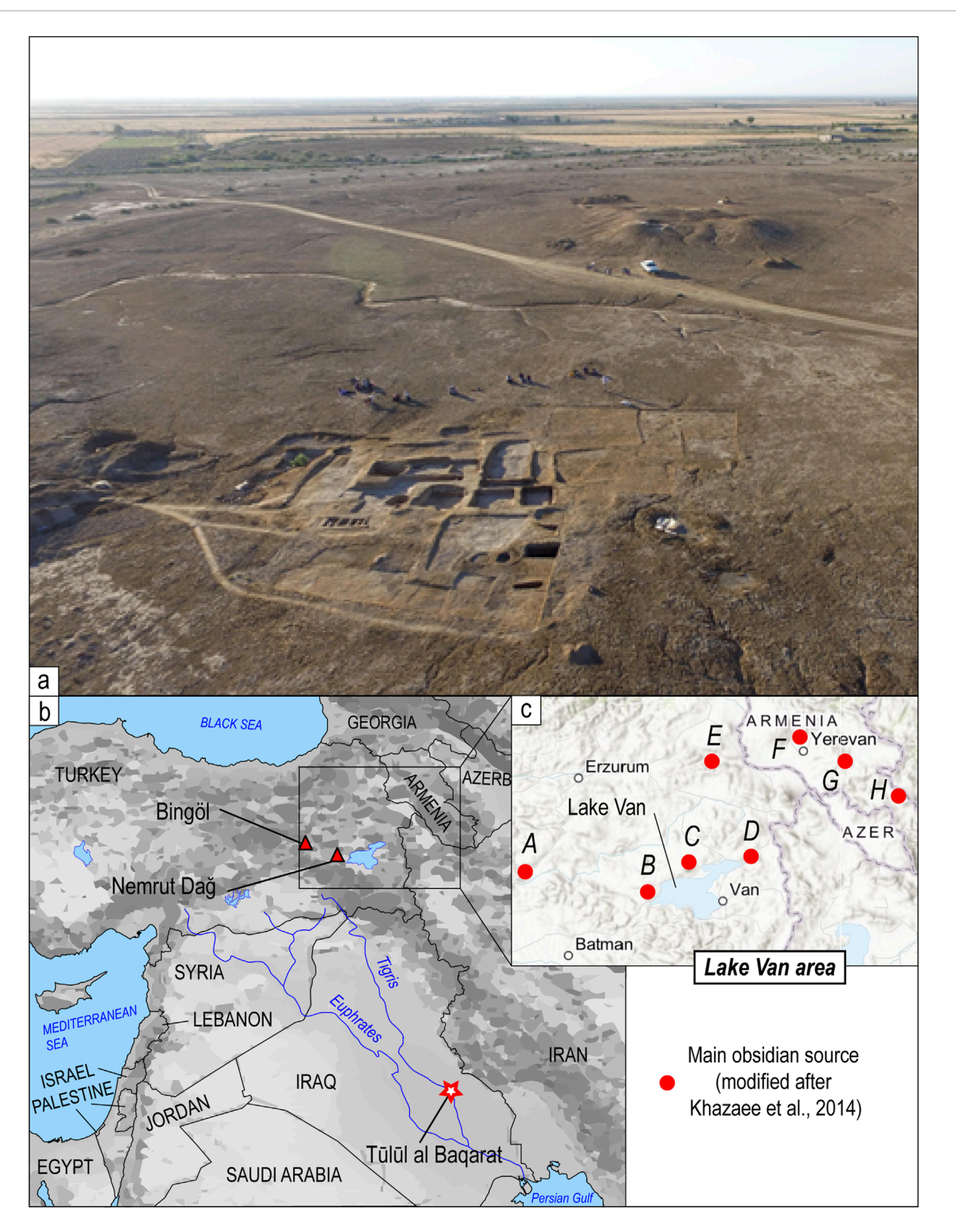


FIGURE 1
(a) Aerial view of the TB7 tell at the Tulūl al-Baqarat archaeological site, the site of discovery of the obsidian tools object of study. (b) Geographic map of the Near East area between Turkey, Armenia, Azerbaijan, and Iraq. The Tulūl al-Baqarat archaeological area is indicated by a red star. (c) Detail of the map in (b), along the Turkey and Armenia border, in the Lake Van area, showing the regional sources of obsidian (modified after Khazaee et al., 2014). Obsidian sources: (A) Bingöl, (B) Nemrut Dağ, (C) Suphan Dağ, (D) Meydan Dağ, (E) Sarikamis, (F) Gutansar, (G) Geghasar, and (H) Syunik.

2025; Figure 1c). The Nemrut Dağ Volcano and Bingöl Plateau offer a wide area of investigation, due to their widespread volcanic activity, wherein the occurrence of numerous obsidian deposits is well known (Innocenti et al., 1976; 1980; Poidevin, 1998; Khazaee et al., 2014; Robin et al., 2015; Robin et al., 2016; Frahm, 2020; Frahm and Carolus, 2022; Frahm, 2023; Frahm, 2025). The Nemrut Dağ stratovolcano and Bingöl Plateau occur in the Lake Van area of south-eastern Anatolia (A, B; Figure 1c).

Detailed volcanological, geological, and geochemical characterization of each obsidian-bearing outcrop is the key to unraveling the source of the Tulūl al-Baqarat tools.

In the archaeological literature, Nemrut Dağ is considered one of the most important sources of raw obsidian used by prehistoric societies for producing tools. However, this does not provide any information about the stratigraphy of most of the obsidian outcrops (Robin et al., 2016).

Nemrut Dağ is an active stratovolcano with a typical effusive activity, which experienced historical eruptions (Aydar et al., 2003; Peretyazhko and Savina, 2017; Ulusoy et al., 2019). This stratovolcano is constituted of a wide caldera (~25 km in diameter, Bigazzi et al., 1994; 1997), partially occupied by a lake, near the southwestern tip of Lake Van (Karaoğlu et al., 2005). Nemrut Dağ stratovolcano was characterized by a polyphase eruptive activity (Özdemir et al., 2006), whose volcanic products, among others, include wide obsidian layers, present at each stage of its activity. The post-caldera activity of the volcano is marked by peralkaline rhyolitic (comendite) intra-caldera lava flows and explosive hydrovolcanic activities. Obsidian deposits related to this eruptive stage and outcropping inside the caldera date between 30 ka (Matsuda et al., 1990) and 15 ka (Cubukçu et al., 2012).

The Bingöl volcanic complex is a basaltic plateau with a thickness of up to 1000 m of effusive rocks (Kurum and Baykara, 2020). These are characterized by a suite of calc-alkaline to weakly alkaline lavas and pyroclastites. Here, two obsidian varieties were recognized, known as "Bingöl-A" and "Bingöl-B" (Cauvin et al., 1986; Cauvin et al., 1991; Bigazzi et al., 1997; Frahm, 2012; Carter et al., 2013).

Frahm (2012) reports the best representative available dataset of georeferenced Nemrut Dağ and Bingöl obsidians, based on geochemical data of 100 obsidian samples. According to Frahm (2012), eleven obsidian outcrops were identified inside and outside of the Nemrut caldera, which were geochemically grouped in six clusters (Nemrut1–6), suggesting the occurrence of rhyolites from calc-alkaline (Nemrut1) to variably alkaline (Nemrut2–5), to the Fe-rich and Al-poor rhyolite variety (Nemrut6; Frahm, 2012).

These georeferenced obsidian clusters, with geochemical characterization, represent a perfect comparison for obsidian geochemistry and a solid base for the database used as a reference for the following machine learning application.

3 Materials and methods

Various micro-analytic, non-invasive, and non-destructive techniques were applied to the compositional study of the nine

obsidian tools. Then, preliminary geochemical comparisons and principal component analysis (PCA: covariate matrix) modeling were done to fully characterize our samples and identify the geochemical fingerprint. In the final step, we applied a machine learning approach, comparing the obtained chemical data with training datasets from the literature.

3.1 Analytical techniques

Major and minor elements of the nine obsidian samples (Figure 2a) were determined using a scanning electron microscope (SEM - JEOL IT300LV) equipped with an energy dispersive microanalysis system (SDD EDS detector-AZtec Oxford Instruments), operating under low-vacuum conditions, which allows for obtaining reliable analysis with a non-invasive and non-destructive approach. Samples were analyzed as they are, without any manipulation or carbon coating. The tools were placed on a glass holder and fixed with putty and conductive carbon tape (Figure 2b). The possibility of operating in a completely non-invasive way represents a non-negligible incentive to the development of specific analytical protocols for applications to the heritage of cultural and archaeological interest.

The operating conditions were acceleration voltage 30 kV, low vacuum 50 Pa, beam current 5 nA, working distance 10 mm, and counting time from 100 s to 300 s. The compositional homogeneity of each tool was verified by quartering the sample surface and acquiring one X-ray elemental map of approximately 1 mm² (total area of 4 mm²) on each quarter. Each map was acquired by avoiding small holes, cracks, scratches, and microlites (Figures 2c,d). The software used for the elemental acquisition was Aztec Oxford Instrument $^{\circledR}$, Features package.

From each area, the sum spectrum was extracted and then quantified with Oxford Instruments AZtec QuantMap: mean and standard deviation were calculated by element. Primary and secondary standards used for EDS quant calibration, and the controls were the minerals from Astimex Scientific Limited[®] 53 Minerals Mount.

The detection and quantification of trace elements were obtained by a benchtop EDAX-Eagle micro-fluorescence (micro-XRF). The micro-XRF uses a beam of collimated polychromatic X-rays to produce the characteristic X-rays of the chemical elements in conditions of high analytical sensitivity that allows for measuring contents lower than 1000 ppm, always in a non-destructive mode (Vaggelli and Cossio, 2012). The analytical conditions of the micro-XRF were an acceleration voltage of 40 kV, a beam current of 1 mA, a counting time of 1000 s, and an XRF beam spot of 30 μm . A 250- μm -thick aluminum foil was used as the primary filter, and the correction method "Fundamental Parameter" with internal standards was applied for the quantitative results, using two reference standards for glass materials: NIST610 and NIST612 (more details in Vaggelli et al., 2013).

Trace elements were determined as a profile of ten spot analyses performed along the elongation of each tool, avoiding small holes, cracks, scratches, and microlites.

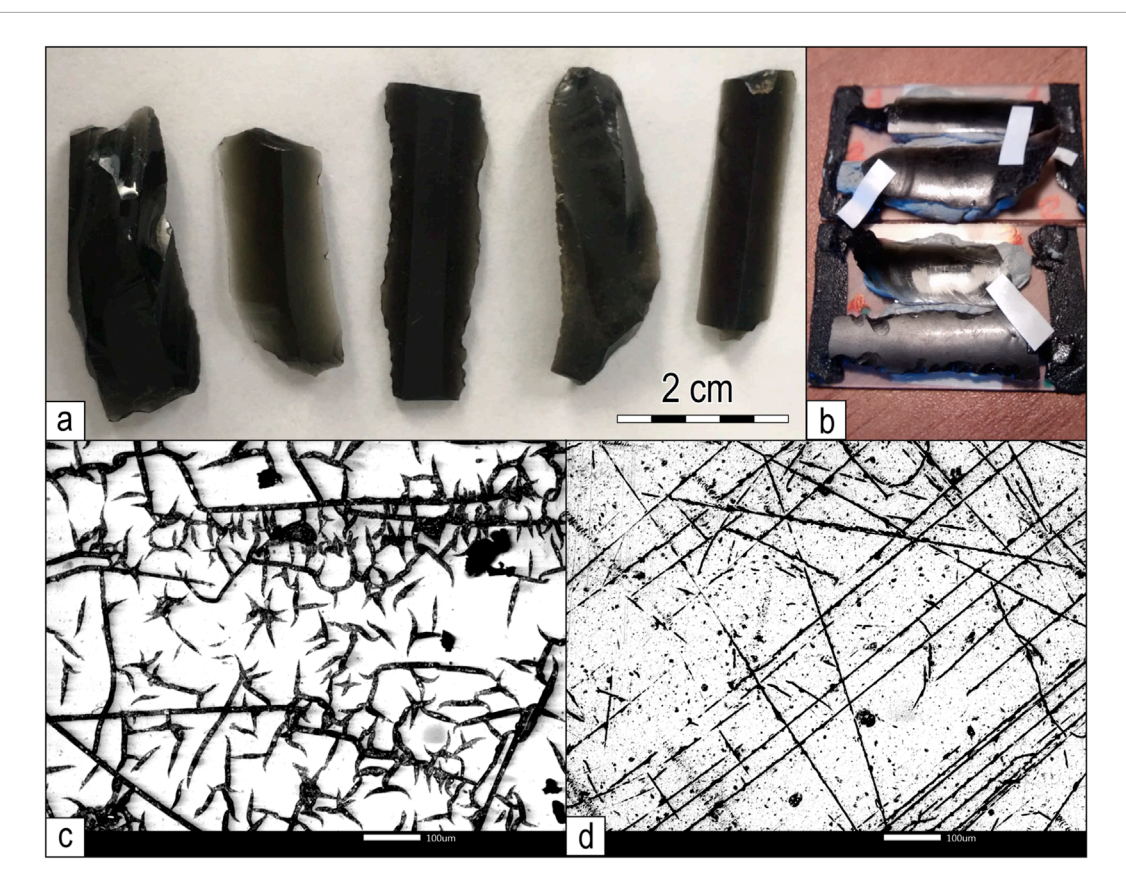


FIGURE 2
(a) Macroscopic picture of five of the nine obsidian tools. (b) Obsidian tools fixed on a glass holder for geochemical measurements. Backscattered electron (BSE) images of the tool surface, highlighting (c) surface cracks and (d) scratches, which were avoided during the measurements.

3.2 Machine learning: decision tree and random forest

To test the machine learning procedure, we built a training dataset of obsidian geochemical data to compare with our geochemical data. Frahm (2012) provides the best representative available dataset, based on electron microprobe analyses, containing 108 georeferenced Nemrut Dağ and Bingöl obsidians, grouped in classes and occurring in different outcrops with similar geochemical imprints.

An applied machine learning approach is based on two well-known algorithms, decision tree (Quinlan, 1986) and random forest (Breiman, 2001).

Decision tree is a top-down classification algorithm (Quinlan, 1986) that constructs tree-like graphs, based on two abstractions: nodes and branches. Branches simply connect nodes with each other, while nodes make decisions, sending an instance to another node (child node) that is connected through a branch. Alternatively, they can return the estimated class of an instance. In the first node (i.e., root), all instances are used to determine the best attribute for splitting the instances into two subsets assigned to two new child nodes. This process is recursively repeated in each new node until the class of all instances of the subset is unique or until a stopping criterion is reached. The best attribute is determined in each node by evaluating the information gain or Gini index.

Random forest (Breiman, 2001) is a meta-classifier (or ensemble) algorithm that trains several decision trees on various subsamples of the original dataset and uses averaging to improve the predictive accuracy and control over-fitting.

Random forest is an ensemble learning method for classification that operates by constructing a multitude of decision trees (Quinlan, 2014) at training time. The output of the random forest is the class selected by the most trees (Breiman, 2001). Random forest can assign importance to the different attributes of a dataset.

In addition, this algorithm is also one of the most cited classifiers for its best results, which makes it interesting to study it in this context.

The random forest calculations were performed by means of SharpLearning (2025) (an open-source machine learning (ML) library for C#.NET, https://github.com/mdabros/SharpLearning). To obtain the best results, we used the RandomSearchOptimizer function, present in the SharpLearning package, to tune hyperparameters. For this optimization, we randomly split the learning database (i.e., Frahm, 2012; containing 108 observations, seven output classes), assigning 70% of the observations to the training dataset and 30% to the test dataset. The optimization run gave the following optimized parameters: trees = 100; maximumTreeDepth = 30; minimumInformationGain = 1.E–06; featuresPrSplit = 0; and minimumSplitSize: = 1 for the random forest algorithm.

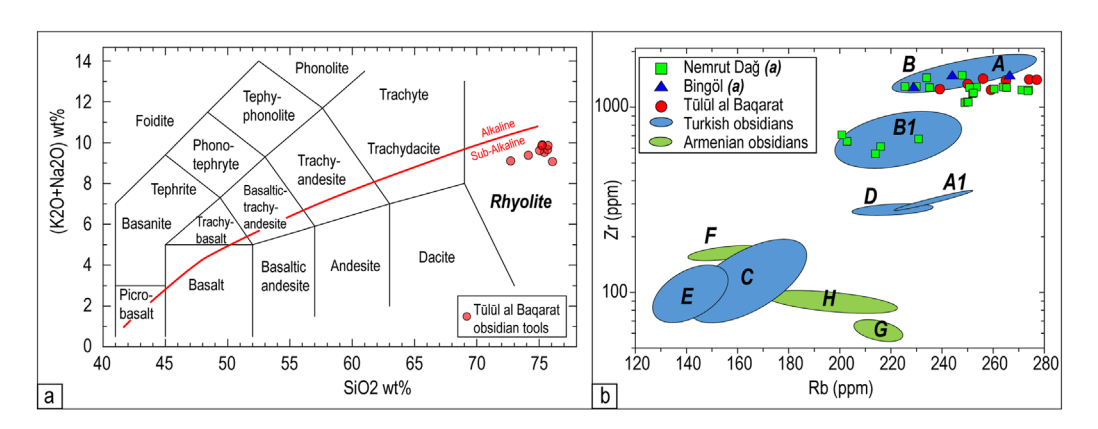


FIGURE 3
(a) Total-alkali vs. silica (TAS, after Le Bas et al., 1986) classification diagram showing the composition of the nine Tulūl al-Baqarat obsidians. The red line represents the geochemical distinction based on the alkali content, after Irvine and Baragar (1971). (b) Rb vs. Zr diagram for obsidians from Turkey (pale blue areas: A: Bingöl-A; A1: Bingöl-B; B: Nemrut Dağ; B1: Nemrut Dağ; C: Suphan Dağ; D: Meydan Dağ; E: Sarikamis) and Armenia (green areas: F: Gutansar; G: Geghasar; H: Syunik) volcanic complexes (modified after Ghorabi et al., 2010; Khazaee et al., 2014). A selection of georeferenced obsidian samples from Nemrut Dağ and Bingöl (Frahm, 2012) is plotted with Tulūl al-Baqarat tools for direct comparison (legend reported in the figure).

Using these parameters, we get a test error, defined as metric error between the known targets test set and test predictions, of <0.05. The returned output includes a list of probabilities (1 for each output class) where the highest value corresponds to the most probable phase.

The algorithm must be trained by associating the input variables (in our case, the concentrations of the elements) with the class they belong to. From here on, it is possible to enter input variables (concentrations of elements in an unknown sample) to obtain the most probable class, that is, the probability (0/1) of belonging, for each available class. A similar procedure was applied to microprobe analysis, and its classification and plotting were described by Cossio et al. (2024).

4 Results and discussion

4.1 Geochemical data of Tulūl al-Baqarat obsidian tools

The representative compositions of each analyzed obsidian (Supplementary Table S1) are first plotted into the TAS diagram (Le Bas et al., 1986), which is based on silica (SiO $_2$) versus total alkali (Na $_2$ O + K $_2$ O), commonly used for the chemical classification of volcanic rocks. As reported in Figure 3a, the analyzed samples indicate a rather homogeneous rhyolite composition.

The material used for carving the nine tools is therefore a natural volcanic glass, showing a high silica content with a peraluminous feature [Al $_2$ O $_3$ / (Na $_2$ O + K $_2$ O + CaO) > 1]. The alkaline content (Na $_2$ O+ K $_2$ O, occurring in similar amounts) is close to 10 wt%. In addition, the alumina (Al $_2$ O $_3$ approximately 11 wt%) and Fe (FeO approximately 2.5 wt%) contents are low, as are the calcium and magnesium (MgO and CaO <1 wt%) contents.

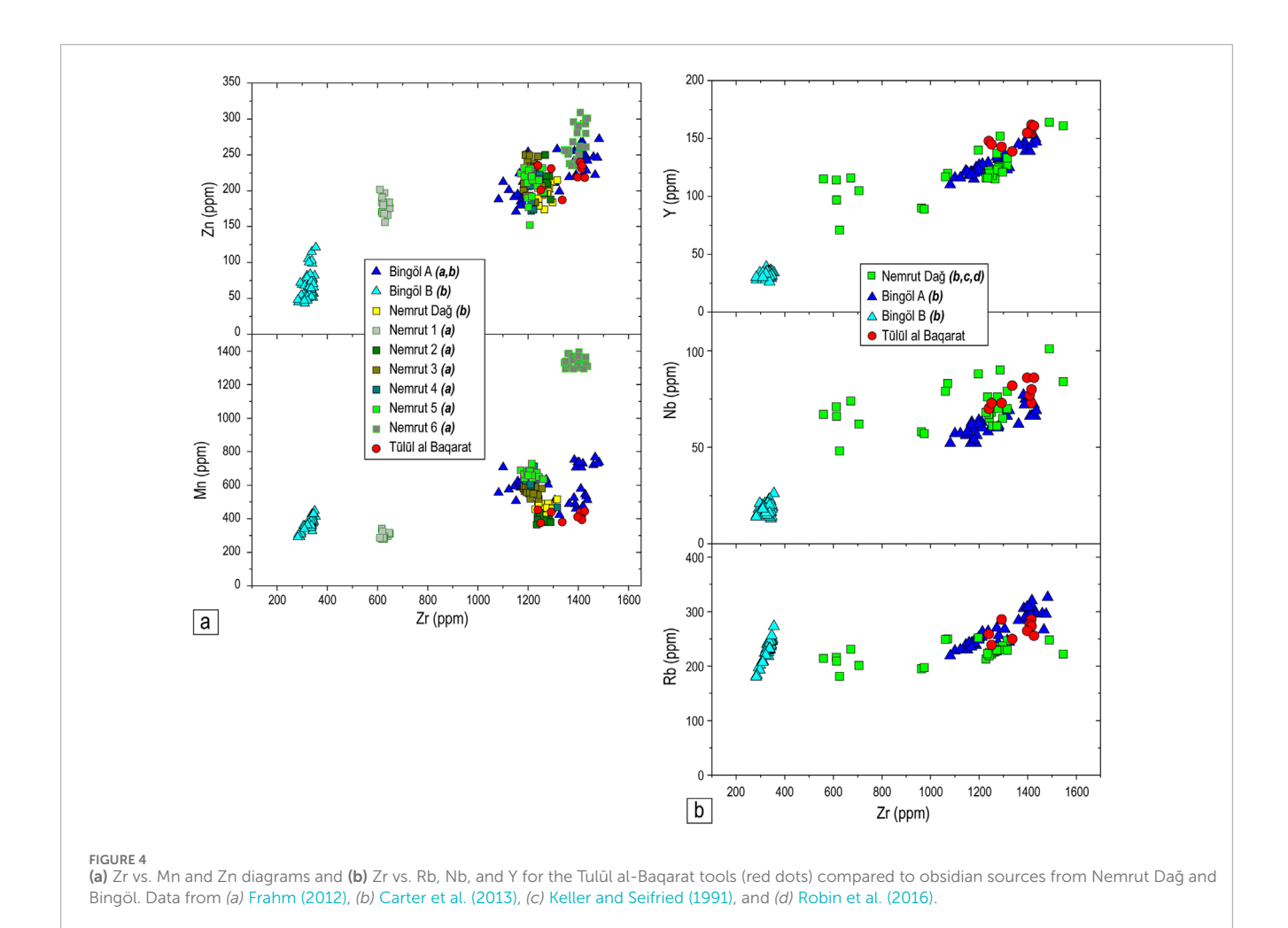
Trace elements show a very high content of Zr (>1000 ppm), together with high values of Rb (200–300 ppm), Y (140–150 ppm), Nb (50–80 ppm), and Zn (150–200 ppm). These values are peculiar features reflecting intraplate

acid volcanic rocks (Le Maitre, 2002) occurring in eastern Anatolia (Innocenti et al., 1982; Di Giusepppe et al., 2017; Peretyazhko et al., 2015). Supplementary Table S1 reports the representative averaged chemical compositions (with relative standard deviation, δ) of the multiple analyses performed for major (i.e., > 1 wt% oxide) and minor (i.e., < 1% wt% oxide) elements on each tool. The detected trace elements (Mn, Ti, Zn, Y, Zr, Nb, and Rb) are similarly reported as average values and relative standard deviation.

4.2 Geochemical comparison of Tulūl al-Baqarat samples with obsidian sources from eastern Turkey and Armenia

The measured chemical compositions of the nine obsidian blades are here compared with those measured on other obsidians from the most widespread Turkish and Armenian obsidian-bearing volcanic areas reported in the literature (Keller and Seifried, 1991; Khademi Nadooshan et al., 2013; Khazaee et al., 2014; Darabi and Glascock, 2013). We have restricted our geochemical consideration to the most significant and analytically best constrained elements, that is, Zr and Rb, which have a remarkable discriminatory capacity in large volcanic contexts. In the Rb vs. Zr plot (Figure 3b), the nine obsidian tools show high values of both Zr and Rb, similar to some Turkish obsidians (A, B in Figure 3b), especially those belonging to Bingöl and Nemrut Dağ. These values are clearly different from all the Armenian (F, H, G in Figure 3b) and other Turkish (C, D, E A1 in Figure 3b) obsidians that are characterized by minor Zr (of one order of magnitude) and Rb (from 60 ppm to 140 ppm less) contents. Therefore, among the possible source areas for the analyzed obsidian tools, only the obsidians from Nemrut Dağ and Bingöl show comparable Zr and Rb values (Figure 3b).

Therefore, an accurate comparison with obsidians that erupted from the Nemrut Dağ stratovolcano and the Bingöl Plateau was performed to evaluate the geochemical fingerprint.



Following this assumption and in agreement with literature studies on Bingöl and Nemrut Dağ obsidians, a set of geochemical diagrams was created using the available data of obsidian sources (Keller and Seyfried, 1990; Frahm, 2012; Sumita and Schmincke, 2013; Carter et al., 2013; Schmincke and Sumita, 2014; Robin et al., 2016). The separation in classes by accurate geochemical analyses of specific chemical elements is the key to identifying the geochemical fingerprint.

We selected Zr vs. Zn, Mn, Rb, Nb, and Y trace element pairs to discriminate the geochemical fingerprints of each volcanic complex, as reported in Figure 4. Unfortunately, these diagrams show a scarce discriminating capacity, contrary to other cases (Khademi Nadooshan et al., 2013; Khazaee et al., 2014). Indeed, in the diagram, Zr vs. Zn and Mn show a clear separation between Bingöl-B, Nemrut1, and Nemrut6 clusters, but it is impossible to distinguish between the Nemrut2–5, Bingöl-A, and Tulūl al-Baqarat obsidians (Figure 4a). Similarly, when comparing Zr vs. Nb, Y, and Rb, an indistinct dataset gathers Nemrut, Bingöl-A, and Tulūl al-Baqarat obsidian samples (Figure 4b).

No clear and exhaustive information was obtained by simple geochemical comparison, and therefore, a further discriminative attempt was performed by applying a machine learning model based on literature data from Frahm (2012) as a training dataset.

4.3 Principal component analysis (PCA)

To verify the good clustering proposed by Frahm (2012), a principal component analysis (PCA) was first applied to these geochemical clusters (Figure 5).

An accurate selection of elements was made for testing PCA, according to their quantitative occurrence (similar order of magnitude) and geochemical behavior.

Two different training sets of geochemical elements were selected to validate the proposed method of attribution according to the available dataset.

The chemical elements for PCA include five major elements (Si, Al, Na, K, and Fe; Supplementary Table S1) for the first dataset, and two minor (Ti and Mn) elements, as well as Zr and Zn, for the second one.

Given the low dimensionality (five elements for major and four for minor/trace), it is possible to represent the analytical points using the mean of the covariance matrix, using the first two PCA components (Figure 5a for major; Figure 5b for minor/trace elements). In these conditions, we have more than 85% of the available variance for the two datasets. In each class, the ellipse represents a deviation of 2 sigma, with respect to the class centroid, projected into the two PCA components. The clear separation and the good grouping between the

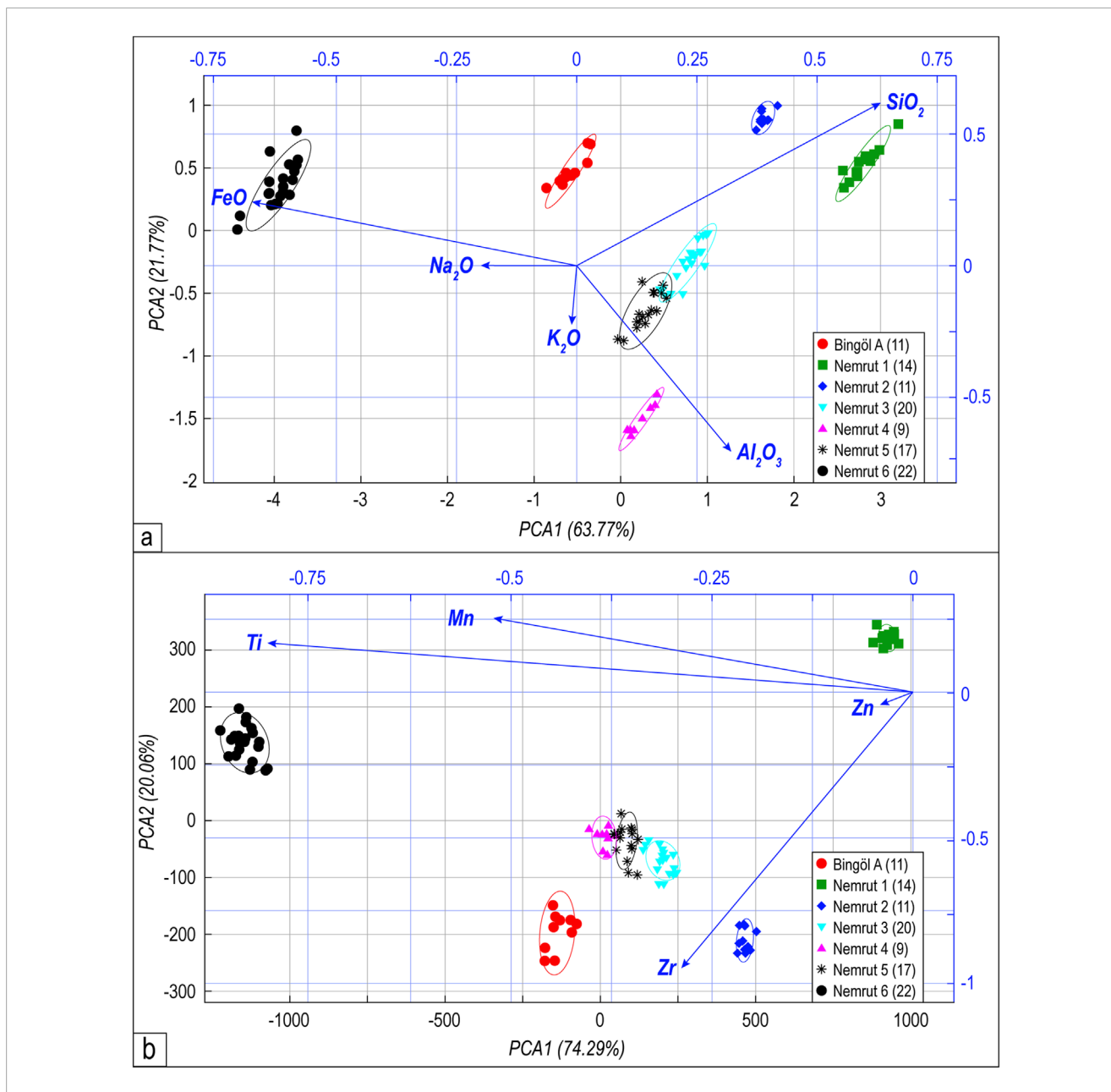


FIGURE 5
Principal component analysis (PCA) on (a) major (Si, Al, Na, K, and Fe) and (b) selected minor/trace (Ti, Mn, Zr, and Zn) elements for Bingöl-A and Nemrut Dağ Obsidians clusters from Frahm (2012). The numbers in brackets are the number of samples in the cluster. The average values of elements for each class (centroid) and relative standard deviations are reported in Supplementary Tables S2, S3.

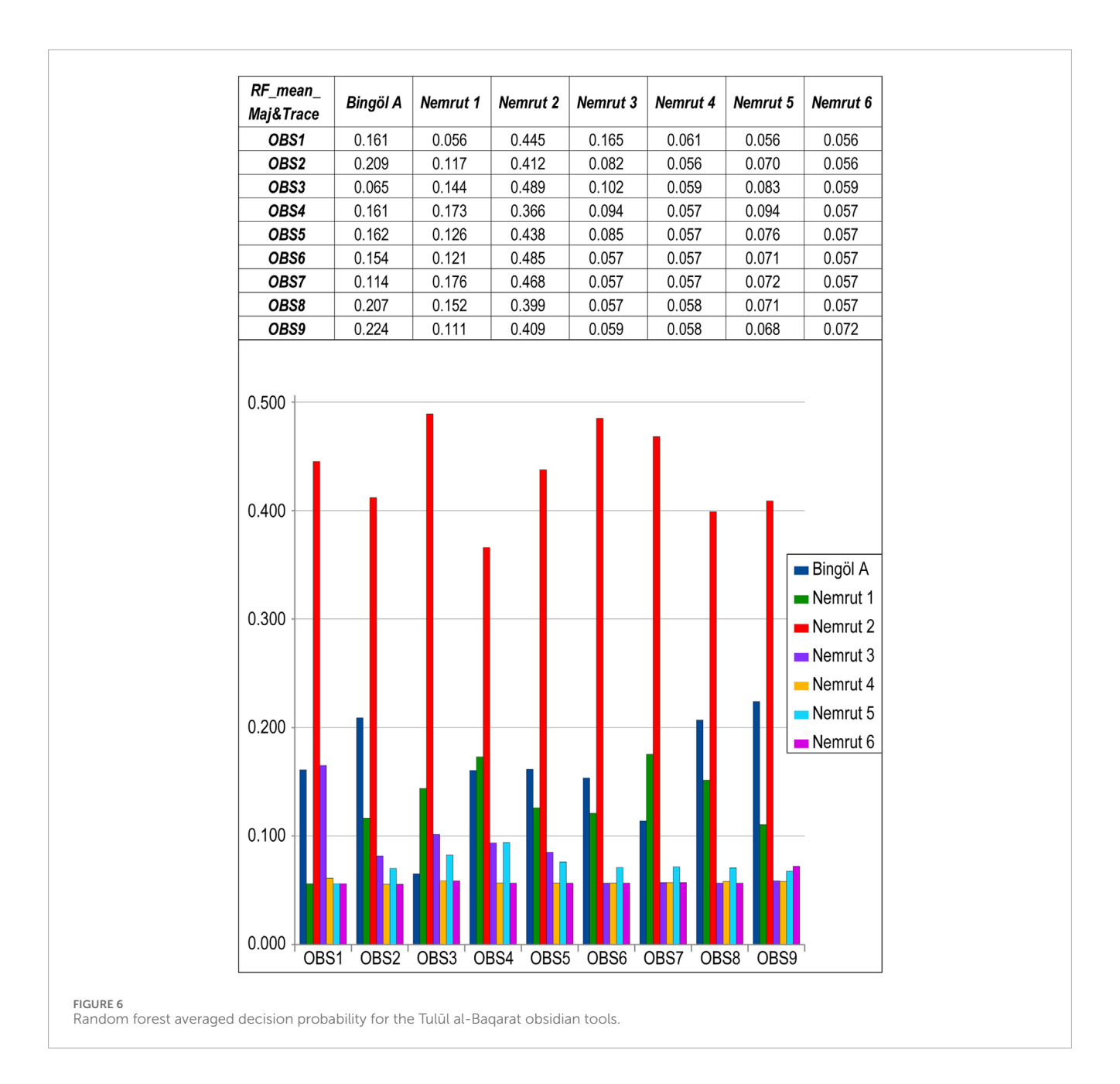
different considered classes allow us to use this information to train the machine learning algorithms with the Frahm (2012) dataset.

4.4 The machine learning approach

After the successful PCA and the resulting good subdivision into database classes (Frahm, 2012), we used this information to train machine learning algorithms based on the random forest algorithm (Quinlan, 2014). Therefore, a detailed comparative study with obsidian samples from different outcrops was performed.

We selected the same chemical elements as for PCA: five major elements (Si, Al, Fe, Na, and K) and four minor/trace elements (Ti, Mn, Zr, and Zn), for both our geochemical data and for the database. Figure 6 shows the histogram of provenance probability, calculated as an average value from major and minor/trace elements probability of belonging to each class present in the database (Bingöl-A and Nemrut1–6), for each obsidian tool.

The results are surprisingly coherent, identifying a statistically significant unique provenance, that is, the Nemrut2 cluster (Figure 6). This cluster shows a statistically significant geochemical affinity to the measured obsidians of Tulūl al-Baqarat, more than



twice that of the second similar cluster (Bingöl-A), while other clusters show a significantly lower statistical affinity (Figure 6).

Nemrut 2 corresponds to an outcrop inside the caldera of Nemrut Dağ Volcano (the EA25 outcrop in Frahm, 2012) and is likely to be the statistically more plausible source rock among the other obsidians.

4.5 Final remarks: the obsidian source

The calculated averaged probability led us to collocate the source rocks of the studied nine obsidian tools in the Nemrut

Dağ stratovolcano (Lake Van region, Turkey), and, more precisely, in the obsidians outcropping inside the caldera, emplaced during the post-caldera activity of Nemrut Dağ Volcano from the last 30 ka (Ulusoy et al., 2012).

The suggested exhaustive hypothesis appears plausible even assuming their transport to the outcrop (i.e., the site of discovery in ancient times) through the main waterways of the region, such as the Tigris River.

This archaeometry study of obsidian sourcing for Tulūl al-Baqarat tools suggests a significant network of interactions among populations of Southeastern Anatolia and the south Near East during the 4th millennium BCE.

5 Conclusions

The results of this study demonstrate that geochemistry is essential in archaeometric research for determining the provenance of raw materials used in the production of artifacts in historical periods. It is here evidenced that geochemical analysis, combined with a machine learning approach, represents a useful procedure for easily distinguishing among different obsidian deposits, reaching, in some cases, the outcrop-scale of detail.

The obsidian tools found in Tulūl al-Baqarat show a composition that is clearly different from other obsidians present in the mid-East (Armenia and central or western Turkey) and are comparable to the volcanic glasses from the Nemrut Dağ Volcano in southeastern Turkey. In more detail, using the procedure presented above, we identified a restricted area (i.e., the caldera) of the Nemrut Dağ Volcano as the most suitable source of the obsidian raw material, from the geochemical point of view. This is the "geochemical fingerprint."

It must be pointed out that element pairs such as Zr vs. Rb, Zr vs. Zn, and Zr vs. FeO (Figure 4) have a roughly discriminating capacity for most Anatolia obsidian sources, because of some geochemical affinities. A machine learning approach was remarkably successful at exhaustively discriminating among similar petrogenetic sources, such as Nemrut and Bingöl.

In conclusion, data obtained in this archaeometric study through non-invasive and non-destructive geochemical analyses and through a machine learning approach suggest that the obsidian deposits were very important as an obsidian source for the production of tools and artifacts by prehistoric populations across the Near East (see, e.g., Muşkara and Konak, 2021; Muskara and Ağırsoy, 2023).

We can also assert that obsidian tool production was not only for local or regional production in the neighborhood of the Nemrut Dağ volcanic area but was part of a larger regional trade network in obsidian and obsidian tools (Khalidi and Gratuze, 2013; Orange et al., 2021).

Indeed, beginning in 9600 BP, this obsidian is only present in the upper Tigris and upper Euphrates basins and followed the diffusion of the calc-alkaline variant (Bingöl-B) toward the middle Euphrates (Gratuze et al., 1993).

Concerning the form in which these raw materials were obtained, it is more likely that this obsidian was accessed directly, being decorticated at source as a means of both testing raw material quality and diminishing transport weight (Carter et al., 2020). As for the question of how the obsidian was moved to Tulūl al-Baqarat, the means of transport were by foot, with the domestication of pack animals, or on a boat. The Nemrut Dağ volcanic area is roughly 1200 km (in a straight line), far from the Tulūl al-Baqarat archaeological site, suggesting a far distance provenance and sourcing. This information provides a more solid comprehension of the trade and exchange network among populations of Southeastern Anatolia and the south Near East during the 4th millennium BCE.

Finally, the reconstruction of the extraordinary influence of the Tigris River in the Near East is emphasized as a route for the transportation of materials toward the shores of the Persian Gulf.

This study provides an important constraint for further archaeological studies on prehistoric settlements in the Middle East and Mediterranean regions.

Data availability statement

The original contributions presented in the study are included in the article/Supplementary Material; further inquiries can be directed to the corresponding author.

Author contributions

GV: Conceptualization, Investigation, Writing – original draft, Writing – review and editing. RC: Formal Analysis, Methodology, Software, Writing – review and editing. AB: Resources, Supervision, Validation, Writing – review and editing. CL: Resources, Supervision, Validation, Writing – review and editing. SG: Data curation, Investigation, Methodology, Visualization, Writing – review and editing.

Funding

The authors declare that financial support was received for the research and/or publication of this article. Financial support was provided by CNR-IGG Torino and by the University of Turin through the Dipartimento di Scienze della Terra. The authors thank the Interdepartmental Centre "G. Scansetti" (University of Turin) for providing access to the μ -XRF laboratory.

Acknowledgements

The authors thank CNR-IGG and the Dipartimento di Scienze della Terra of Turin University for supporting the geochemical analyses of the present study. The senior author is grateful to Ellery Frahm for the critical reading of an early version of the manuscript and for suggestions.

Conflict of interest

The authors declare that the research was conducted in the absence of any commercial or financial relationships that could be construed as a potential conflict of interest.

Generative AI statement

The authors declare that no Generative AI was used in the creation of this manuscript.

Any alternative text (alt text) provided alongside figures in this article has been generated by Frontiers with the support of artificial intelligence and reasonable efforts have been made to ensure accuracy, including review by the authors wherever possible. If you identify any issues, please contact us.

Publisher's note

All claims expressed in this article are solely those of the authors and do not necessarily represent those of their affiliated

organizations, or those of the publisher, the editors and the reviewers. Any product that may be evaluated in this article, or claim that may be made by its manufacturer, is not guaranteed or endorsed by the publisher.

References

Alıcı, P., Temel, A., Gourgaud, A., Vidal, P., and Gündogdu, M. N. (2001). Quaternary tholeitic to alkaline volcanism in the karasu valley, dead sea rift zone, southeast Turkey: Sr-Nd-Pb-O isotopic and trace-element approaches to crust-mantle interaction. *Int. Geol. Rev.* 43, 120–138. doi:10.1080/00206810109465004

Alpaslan, M. (2007). Early to middle Miocene intra-continental basaltic volcanism in the northern part of the Arabian plate, SE Anatolia, Turkey: geochemistry and petrogenesis. *Geol. Mag.* 144 (5), 867–882. doi:10.1017/s0016756807003524

Aydar, E., Gourgaud, A., Ulusoy, I., Digonnet, F., Labazuy, P., Şen, E., et al. (2003). Morphological analysis of active mount nemrut stratovolcano, eastern Turkey: evidences and possible impact areas of future eruption. *J. Volcanol. Geotherm. Res.* 123, 301–312. doi:10.1016/s0377-0273(03)00002-7

Azizi, H., and Tsuboi, M. (2021). The Van microplate: a new microcontinent at the junction of Iran, Turkey and Armenia. Front. Earth Sci. 29 January 2021. Sec. Petrol. 8, 574385. doi:10.3389/feart.2020.574385

Bahar, A. (2020). Statues and votive vessels from Tulūl al-Baqarāt. Z. für Assyriol. 110 (2), 218–241. doi:10.1515/za-2020-0022

Bahar, A. (2022). Sumerian and akkadian stelae from Tülül -al-Baqarat. Revue d'Assyriologie d'Archéologie Orient. 116, 31–41. doi:10.3917/assy.116.0031

Bak, T., Yağcioğlu, U. C., Şen, C., and Şişman Tükel, F. (2025). Northeast Anatolian obsidians: preliminary results. *Turk. J. Earth Sci.* 34 (3), 440–454. doi:10.55730/1300-0985 1968

Bigazzi, G., and Bonadonna, F. P. (1993). Fission track dating of the obsidian of lipari island (italy). *Nature* 242 (5396), 322–323. doi:10.1038/242322a0

Bigazzi, G., Yegingil, Z., Ercan, T., Oddone, M., and Özdogan, M. (1994). Provenance studies of prehistoric artifacts in eastern anatolian: interdisciplinary research results. *Mineral. Petrogr. Acta* 37, 17–36.

Bigazzi, G., Yeğingil, Z., Ercan, T., Oddone, M., and Özdoğan, M. (1997). Age determination of obsidian bearing volcanic s in eastern Anatolia using the fission track dating method. *Geol. Bull. Turk.* 40 (2), 57–72.

Biró, K. (2005). Non-destructive research in archaeology. *J. Radioanal. Nucl. Chem.* 265, 235–240. doi:10.1007/s10967-005-0814-6

Breiman, L. (2001). Random forests. *Mach. Learn.* 45, 5–32. doi:10.1023/a:1010933404324

Carter, T., Grant, S., Kartal, M., Coşkun, A., and Özkaya, V. (2013). Networks and neolithisation: sourcing obsidian from körtik tepe (SE Anatolia). *J. Archaeol. Sci.* 40 (1), 556–569. doi:10.1016/j.jas.2012.08.003

Carter, T., Campeau, K., and Streit, K. (2020). Transregional perspectives: characterizing obsidian consumption at Early Chalcolithic Ein el-Jarba (N. Israel). *J. Field Archaeol.* 45, 249–269. doi:10.1080/00934690.2020.1717857

Cauvin, M. C., Balkan, N., Besnus, Y., and Şaroğlu, F. (1986). Origine de l'obsidienne de Cafer Höyük (Turquie): premiers résultats. *Paléorient* 12 (2), 89–97. doi:10.3406/paleo.1986.4411

Cauvin, M. C., Besnus, Y., Tripier, J., and Montigny, R. (1991). Nouvelles analyses d'obsidiennes du Proche-Orient: modèle de géochimie des magmas utilisé pour la recherche archéologique. *Paléorient* 17 (2), 5–20. doi:10.3406/paleo.1991.4550

Chataigner, C., Poidevin, J. L., and Arnaud, N. O. (1998). Turkish occurrences of obsidian and use by prehistoric peoples in the near east from 14,000 to 6000 BP. J. Volcanol. Geotherm. Res. 85 (1-4), 517–537. doi:10.1016/S0377-0273(98)

Cossio, R., Ghignone, S., Borghi, A., Corno, A., and Vaggelli, G. (2024). A supervised machine learning procedure for EPMA classification and plotting of mineral groups. *Appl. Comput. Geosci.* 23, 100186. doi:10.1016/j.acags.2024.100186

Çubukçu, H. E., Ulusoy, İ., Aydar, E., Ersoy, O., Şen, E., Gourgaud, A., et al. (2012). Mt. Nemrut volcano (eastern Turkey): temporal petrological evolution. *J. Volcanol. Geotherm. Res.* 209–210, 33–60. doi:10.1016/j.jvolgeores.2011.08.005

Darabi, H., and Glascock, M. D. (2013). The source of Obsidian artefacts found at east chia sabz, Western Iran. *J. Archaeol. Sci.* 40 (10), 3804–3809. doi:10.1016/j.jas.2013.04.022

Di Giuseppe, P., Agostini, S., Lustrino, M., Karaoğlu, Ö., Savaşçın, M. Y., Manetti, P., et al. (2017). Transition from compression to strike-slip tectonics revealed by Miocene–Pleistocene volcanism west of the karlıova triple junction (east Anatolia). *J. Petrol.* 58 (10), 2055–2087. doi:10.1093/petrology/egx082

Supplementary material

The Supplementary Material for this article can be found online at: https://www.frontiersin.org/articles/10.3389/feart.2025.1675908/full#supplementary-material

Di Giuseppe, P., Agostini, S., Manetti, P., Savaṣçın, M. Y., and Conticelli, S. (2018). Sub-lithospheric origin of Na-alkaline and calc-alkaline magmas in a post-collisional tectonic regime: Sr-Nd-Pb isotopes in recent monogenetic volcanism of cappadocia, central Turkey. *Lithos* 316–317, 304–322. doi:10.1016/j.lithos.2018.07.018

Frahm, E. (2012). Distinguishing nemrut Dağ and Bingöl A obsidians: geochemical and landscape differences and the archaeological implications. *J. Archaeol. Sci.* 39, 1436–1444. doi:10.1016/j.jas.2011.12.038

Frahm, E. (2020). Variation in nemrut dağ obsidian at pre-pottery Neolithic to late Bronze Age sites (or: all that's nemrut dağ obsidian isn't the sıcaksu source). *J. Archaeol. Sci. Rep.* 32, 102438. doi:10.1016/j.jasrep.2020.102438

Frahm, E. (2023). The obsidian sources of eastern Turkey and the caucasus: Geochemistry, geology, and geochronology. *J. Archaeol. Sci. Rep.* 49, 104011. doi:10.1016/j.jasrep.2023.104011

Frahm, E. (2025). Archaeological obsidian sourcing: looking from the first 60 years to the next. J. Arch. Sci. 177, 106200. doi:10.1016/j.jas.2025.106200

Frahm, E., and Carolus, C. M. (2022). Identifying the origins of obsidian artifacts in the deh luran plain (southwestern Iran) highlights community connections in the Neolithic zagros. *PNAS* 119 (43), e2109321119. doi:10.1073/pnas.2109321119

Ghorabi, S., Khademi Nadooshan, F., Glascock, M. D., Hejabari Noubari, A., and Ghorbani, M. (2010). Provenance of obsidian tools from north-western Iran using Xray fluorescence analysis and neutron activation analysis. *IAOS Bull.* 43, 14–20.

Gratuze, B., Barrandon, J., Al Isa, K., and Cauvin, M. C. (1993). Non-destructive analysis of obsidian artefacts using nuclear techniques: investigation of provenance of near Eastern artefacts. *Archaeometry* 35, 11–21. doi:10.1111/j.1475-4754.1993.tb01020.x

Innocenti, F., Mazzuoli, R., Pasquarè, G., Radicati di Brozolo, F., and Villari, L. (1976). Evolution of volcanism in the area of interaction between the Arabian, Anatolian and Iranian plates, Lake Van, Eastern Turkey. *J. Volcanol. Geotherm. Res.* 1, 103–112. doi:10.1016/0377-0273(76)90001-9

Innocenti, F., Mazzuoli, R., Pasquarè, G., Serri, C., and Villari, L. (1980). Geology of the volcanic area north of Lake Van (Turkey). *Geol. Rundsch.* 69, 292–322. doi:10.1007/BF01869038

Innocenti, F., Mazzuoli, R., Pasquarè, G., Radicati di Brozolo, F., and Villari, L. (1982). Tertiary and Quaternary volcanism of the erzurumkars area (Eastern Turkey): geochronological data and geodynamic evolution. *J. Volcanol. Geotherm. Res.* 13 (3), 223–240. doi:10.1016/0377-0273(82)90052-X

Irvine, T. N., and Baragar, W. R. A. (1971). A guide to the chemical classification of the common volcanic rocks. *Can. J. Earth Sci.* 8, 523–548. doi:10.1139/e71-055

Karaoğlu, Ö., Özdemir, Y., Tolluoğlu, A. Ü., Karabıyıkoğlu, M., Köse, O., and Froger, J. L. (2005). Stratigraphy of the volcanic products around Nemrut caldera: implications for reconstruction of the caldera formation. *Turk. J. Earth Sci.* 14, 123–143.

Kearney, R. J., Goff, J., Smith, V., Schwab, M. J., Özdemir, Y., Karaoğlu, Ö., et al. (2025). Glass geochemistry and tephrostratigraphy of key tephra layers in and around Lake Van, eastern anatolian volcanic province (EAVP). Quat. Sci. Rev. 352, 109165. doi:10.1016/j.quascirev.2024.109165

Keller, J., and Seifried, C. (1991). The present status of obsidian source identification in Anatolia and the near east. Volcanology and archaeology. *Proc. Eur. Work. Ravello, PACT* 25, 57–87.

Keller, J., and Seifried, C. (1990). The present status of obsidian source identification in Anatolia and the Near East. Editors C. Albore Livadie, and F. Wiedemann (PACT) 25, 58e87.

Keskin, M. (2003). Magma generation by slab steepening and breakoff beneath a subduction-accretion complex: an alternative model for collision-related volcanism in eastern Anatolia, Turkey. *Geophys. Res. Lett.* 30, 2003GL018019. doi:10.1029/2003GL018019

Keskin, M., Pearce, J. A., and Mitchell, J. G. (1998). Volcano-stratigraphy and geochemistry of collision-related volcanism on the Erzurum-Kars Plateau, northeastern Turkey. *J. Volcanol. Geotherm. Res.* 85, 355–404. doi:10.1016/s0377-0273(98)00063-8

Khademi Nadooshan, F., Abedi, A., Glascock, M. D., Eskandari, N., and Khazaee, M. (2013). Provenance of prehistoric obsidian artefacts from kul Tepe, northwestern Iran using X-ray fluorescence (XRF) analysis. *J. Archaeol. Sci.* 40, 1956–1965. doi:10.1016/j.jas.2012.12.032

Khalidi, L., and Gratuze, B. (2013). Late chalcolithic lithic assemblage at tell Hamoukar's southern extension. *Berytus* 53-54 2010-2011, 1–24.

Khazaee, M., Glascock, M. D., Masjedi, P., Khademi Nadooshan, F., Soleimani Farsani, R., Delfan, M., et al. (2014). Sourcing the obsidian of prehistoric tools found in western Iran to south-eastern Turkey: a case study for the sites of eastern chia sabz and chogha ahovan. *Anatol. Stud.* 64, 23–31. doi:10.1017/S0066154614000039

Kurt, M. A., Alpaslan, M., Göncüoğlu, M. C., and Temel, A. (2008). Geochemistry of late-stage medium to high-K calc-alkaline and shoshonitic dykes in the Ulukişla basin (central Anatolia, Turkey): petrogenesis and tectonic setting. *Geochem. Int.* 46, 1145–1163. doi:10.1134/s0016702908110062

Kurum, S., and Baykara, T. (2020). Geochemistry of post-collisional yolçatı (bingöl) volcanic rocks in eastern Anatolia, Turkey. *J. Afr. Earth. Sci.* 161, 103653. doi:10.1016/j.jafrearsci.2019.103653

Le Bas, M. J., Le Maitre, R. W., Streckeisen, A., and Zanettin, B. (1986). A chemical classification of volcanic rocks based on the total alkali-silica diagram. *J. Petrology* 27 (3), 745–750. doi:10.1093/petrology/27.3.745

Le Maitre, R. W. (2002). Igneous rocks. A classification and glossary of terms (Cambridge: Cambridge University Press), 236.

Lippolis, C. (2020). L' Area Archeologica di Tülül Al-Baqarat. Gli scavi della missione italiana. *Apice libri - Sesto Fiorent. (Firenze)* I and II, 454.

Lippolis, C., Quirico, E., Bruno, J., Ragazzon, G., Hasanian, A., Kazai, S., et al. (2019). Tulul al-Baqarat, mound 7 (TB7). Preliminary report (season 2015-2018). *Sumer* LXV, 132–163

Lustrino, M., Keskin, M., Mattioli, M., Lebedev, V. A., Chugaev, A., Sharkov, E., et al. (2010). Early activity of the largest Cenozoic shield volcano in the circum-Mediterranean area: mt. Karacada g, SE Turkey. Eur. J. Mineral. 22, 343–362. doi:10.1127/0935-1221/2010/0022-2024

Lustrino, M., Salari, G., Rahimzadeh, B., Fedele, L., Masoudi, F., and Agostini, S. (2021). Quaternary melanephelinites and melilitites from nowbaran (NW urumiehdokhtar magmatic arc Iran): origin of ultrabasic-ultracalcic melts in a post-collisional setting. *J. Petrol.* 62 (9), egab058. doi:10.1093/petrology/egab058

Matsuda, J. I., Ui, T., Notsu, K., Nagao, K., Kita, I., Fujitani, T., et al. (1990). "Geochemical study of collision volcanism at the plate boundary in Turkey (comparison with subduction volcanism in Japan)," in *Initial report on geochemical data, Turkey-Japan volcanological project part II*, 71.

Muşkara, Ü., and Konak, A. (2021). Obsidian source identification at gre Filla, Turkey. J. Archaeol. Sci. Rep. 38, 103003. doi:10.1016/j.jasrep.2021.103003

Muskara, U., Ağırsoy, Z. B., and Beyza Ağırsoy, Z. (2023). Obsidian production strategies at Kendale Hecala during the Neolithic and Ubaid periods. *J. Archaeol. Sci. Rep.* 49, 104039. doi:10.1016/J.JASREP.2023.104039

Oddone, M., Yegingil, Z., Ozdogan, M., Meloni, S., and Bigazzi, G. (2003). Provenance studies of obsidian artefacts from Turkish Neolithic sites using an interdisciplinary approach INAA and fission Track Dating. *Rev. d'Archeometrie* 27, 137–145. doi:10.3406/arsci.2003.1049

Orange, M., Le Bourdonnec, F.-X., Berthon, R., Mouralis, D., Gratuze, B., Thomalsky, J., et al. (2021). Extending the scale of obsidian studies: towards a high-resolution investigation of obsidian prehistoric circulation patterns in the southern caucasus and north-western Iran. *Archaeometry* 63 (3), 923–940. doi:10.1111/arcm.12660

Özdemir, Y., Karaoğlu, Ö., Tolluoğlu, A. U., and Güleç, N. (2006). Volcanostratigraphy and petrogenesis of the nemrut stratovolcano, east anatolian high Plateau: the most recent post-collisional volcanism in Turkey. *Chem. Geol.* 226, 189–211. doi:10.1016/j.chemgeo.2005.09.020

Özdogan, M. (1994). "Çayônii: the chipped stone industry of the pottery Neolithic layers," in *Neolithic chipped stone industries of the fertile crescent*. Editors H. G. Gebel, and S. K. Kozlowski (Berlin), 267–277.

Pearce, J. A., Bender, J. F., De Long, S. E., Kidd, W. F. S., Low, P. J., Güner, Y., et al. (1990). Genesis of collision volcanism in eastern Anatolia, Turkey. *J. Volcanol. Geotherm. Res.* 44, 189–229. doi:10.1016/0377-0273(90)90018-b

Peretyazhko, I. S., and Savina, E. A. (2017). Processes of the formation of mugearitic and benmoreitic magmas on nemrut volcano (east Turkey). *Dokl. Earth Sci.* 474 (1), 535–541. doi:10.1134/S1028334X17050087

Peretyazhko, I. S., Savina, E. A., and Karmanov, N. S. (2015). Comendites and pantellerites of nemrut volcano, eastern Turkey: genesis and relations between the trachyte-comenditic, comenditic, and pantelleritic melts. *Petrology* 23 (6), 576–622. doi:10.1134/S0869591115060041

Poidevin, J. L. (1998). "Les gisements d'obsidienne de Turquie et de Transcaucasie: géologie, géochimie et chronométrie," in *L'obsidienne au Proche et Moyen-Orient: Du Volcan à l'Outil*. Editors M. C. Cauvin, A. Gourgaud, B. Gratuze, N. Arnaud, G. Poupeau, and J. L. Poidevin (BAR International Series), 105e167.

Quinlan, J. R. (1986). Induction of decision trees. *Mach. Learn.* 1, 81–106. doi:10.1007/bf00116251

Quinlan, J. R. (2014). C4.5: programs for machine learning. Elsevier, 58-60.

Robin, A. K., Mouralis, D., Kuzucuoğlu, A. E., Akkoprü, E., Gratuze, B., Ali Fuat, D., et al. (2015). Les affleurements d'obsidiennes du Nemrut (Anatolie orientale): mise en évidence d'une source exploitable, premiers résultats. *Geomorphology* 21 (3), 217–234. doi:10.4000/geomorphologie.11055

Robin, A. K., Mouralis, D., Akköprü, E., Gratuze, B. C., Kuzucuoğlu, C., Nomade, S., et al. (2016). Identification and characterization of two new obsidian sub-sources in the nemrut volcano (eastern Anatolia, Turkey): the sıcaksu and Kayacık obsidian. *J. Archaeol. Sci. Rep.* 9, 705–717. doi:10.1016/j.jasrep.2016.08.048

Schmincke, H. U., and Sumita, M. (2014). Impact of volcanism on the evolution of lake Van (eastern Anatolia) iii: periodic (nemrut) vs. episodic (suphan) explosive eruptions and climate forcing reflected in a tephra gap between ca. 14 ka and ca. 30 ka. *J. Volcanol. Geotherm. Res.* 285, 195–213. doi:10.1016/j.jvolgeores.2014.08.015

SharpLearning (2025). An open source machine learning library for C#.net. Available online at: https://github.com/mdabros/SharpLearning.

Shaw, J. E., Baker, J. A., Menzies, M. A., Thirlwall, M. F., and Ibrahim, K. M. (2003). Petrogenesis of the largest intraplate volcanic field on the Arabian plate (Jordan): a mixed lithosphere asthenosphere source activated by lithospheric extension. *J. Petrol.* 44, 1657–1679. doi:10.1093/petrology/egg052

Sumita, M., and Schmincke, H. U. (2013). Impact of volcanism on the evolution of lake Van i: evolution of explosive volcanism of Nemrut volcano (eastern Anatolia) during the past >400,000 years. *Bull. Volcanol.* 75, 714. doi:10.1007/s00445-013-0714-5

Tykot, R. H. (1996). Obsidian procurement and distribution in the central and Western mediterranean. *J. Mediterr. Archaeol.* 9 (1), 39–82. doi:10.1558/jmea.v9i1.39

Ulusoy, I., Çubukçu, H. E., Ercan, A., Labazuy, P., Ersoy, O., Şen, E., et al. (2012). Volcanological evolution and caldera forming eruptions of mt. Nemrut (Eastern Turkey). *J. Volcanol. Geotherm. Res.* 245–246, 21–39. doi:10.1016/j.jvolgeores.2012.06.031

Ulusoy, I., Çubukçu, H. E., Mouralis, D., and Ercan, A. (2019). World Geomorphological Landscapes Landscapes and Landforms of Turkey || Nemrut Caldera and Eastern Anatolian Volcanoes: Fire in the Highlands. 589–599. doi:10.1007/978-3-030-03515-0_35

Vaggelli, G., and Cossio, R. (2012). μ -XRF analysis of glasses: a non-destructive utility for cultural heritage applications. *Analyst* 137, 662–667. doi:10.1039/c1an15518k

Vaggelli, G., Lovera, V., Cossio, R., and Mirti, P. (2013). Islamic glass weights from Egypt. *J. Non-Cryst. Solids* 363, 96–102. doi:10.1016/j.jnoncrysol.2012.12.003

Yılmaz, Y., Güner, Y., and Şaroğlu, F. (1998). Geology of the Quaternary volcanic centres of the east Anatolia. *J. Volcanol. Geotherm. Res.* 85, 173–210. doi:10.1016/S0377-0273(98)00055-9